*32nd EPS Conference on Plasma Phys. Tarragona, 27 June - 1 July 2005 ECA Vol.**29C**, O-2.005 (2005)*

Modelling of Power Fluxes during Thermal Quenches

C. Konz, D.P. Coster, K. Lackner, G. Pautasso, and the ASDEX Upgrade Team

Max-Planck Institute for Plasma Physics, 85748 Garching, Germany

EURATOM Association

Introduction

Plasma disruptions are characterised by the sudden loss of magnetic confinement which is followed by high energy fluxes to the plasma facing components (PFCs). They are likely to be unavoidable, at least occasionally, in present day and future tokamaks like ITER. For the latter, parallel energy fluxes of tens of GWm^{-2} to PFCs for timescales of about a millisecond are predicted [1]. Such high energy fluxes can cause substantial damage to PFCs through sublimation of carbon materials as well as melting and evaporation of metals.

We investigate the nature of power fluxes during the thermal quench phase of disruptions by means of numerical simulations with the B2 SOLPS multifluid code which treats ions, electrons, and neutrals as separate species [2]. The simulations are performed in two steps. In a first step, detailed steady-state pre-disruption equilibria are generated based on ASDEX Upgrade Shot #17151 (H-mode shot with neutral beam injection). Power fluxes to the divertors are determined by the power input modelled through ASTRA runs [3] as well as sheath boundary conditions and applied flux limiters for the parallel particle and heat fluxes. The generated equilibria are then subjected to a simulated thermal quench by artificially enhancing the perpendicular transport in the ion and electron channels. This model assumes that the magnetic configuration remains unchanged during the initial phase of the thermal quench (redistribution phase) and the simulation is stopped before the onset of the current quench. Furthermore, radiative losses during the thermal quench are neglected in this first suite of runs. We simulate the entire plasma volume, neutrals are treated as a fluid, and impurities are neglected so far.

The enhanced transport coefficients χ_e, χ_i, and D_n are added to the steady-state values χ_e^0, χ_i^0, and D_n^0 which were obtained through fitting to the ASDEX Upgrade shot #17151 (all of the order of $1\,\mathrm{m}^2\mathrm{s}^{-1}$). They follow the model for electron heat transport in a tokamak with destroyed magnetic flux surfaces [4], i.e. $\chi, D \sim T^{5/2}$. More precisely, we set

$$\chi_\mathrm{e} = f(r)\ \frac{n_\mathrm{e,ref}}{n_\mathrm{e}}\ T_\mathrm{e}^{5/2}\ ,\ \ \chi_\mathrm{i} = f(r)\ \sqrt{\frac{m_\mathrm{e}}{m_\mathrm{i}}}\ \frac{n_\mathrm{i,ref}}{n_\mathrm{i}}\ T_\mathrm{i}^{5/2}\ ,\ \text{and}\ \ D = f(r)\ \sqrt{\frac{m_\mathrm{e}}{m_\mathrm{i}}}\ T_\mathrm{i}^{5/2} \qquad (1)$$

where the reference densities $n_\mathrm{e,ref}$ and $n_\mathrm{i,ref}$ are taken at the outboard midplane separatrix position. The radial factor $f(r)$ is a priori chosen to be constant: $f(r) \equiv 1000$. This first crude model for the enhanced transport coefficients will be improved in the future.

A series of quench runs have been performed, all of which are based on the experimental shot. They differ, however, by the pre-disruptive divertor conditions, i.e. temperatures and densities in the divertor regions prior to the disruption, which play a key role in determining the type of transport in these regions, rather convective or more conductive, and are manipulated in our simulations by varying the puffing rate for fuel neutrals from the wall.

Results

We start our analysis by looking at the timescales of the power fluxes onto the divertors which are experimentally easily accessible. The enhanced cross-field transport leads to a rapid heat pulse on the divertors which can be described by defining a rise time τ_r as the time in which the power on the strike-point modules rises from 15% to 100% of its maximum value during the disruption. In a similar way, a decay time τ_d can be defined by the time in which the strike-point power drops from its maximum value to half of that value.

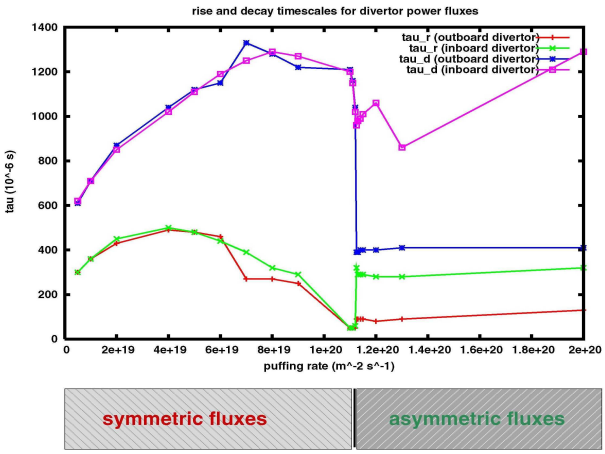

Figure 1: rise and decay times τ_r and τ_d for the total power onto divertors

Fig. 1 shows the rise and decay times for the total power onto divertors for the inboard and outboard divertors vs. the puffing rate Γ.

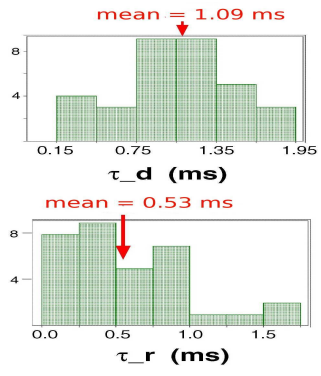

Figure 2: τ_r and τ_d for a dataset of 50 ASDEX Upgrade disruptions [5]

The rise times found in the simulations lie in a range from $\sim 50\,\mu$s to ~ 0.5ms while the decay times range between $\sim 400\,\mu$s and 1.3ms. This agrees rather well with power flux timescales found in a dataset of 50 ASDEX Upgrade disruptions (Fig. 2) although the experimental scatter is somewhat larger. More interesting, however, is the clear dependence of the power flux timescales found in the simulations on the pre-disruptive divertor conditions marked here by the puffing rate. Increasing the rate of neutral puffing from the scrape-off layer (SOL) boundary increases the density in the divertors and thereby lowers the temperature. At a certain puffing rate a clear transition in the timescales can be found in Fig. 1. Analysing the power fluxes to the divertors, we find a transition from equally distributed power fluxes to a

situation where most of the power flux goes to the outboard divertor (asymmetric fluxes). This transition is connected to the increasing fraction of convective heat flux $Q_{\mathrm{conv}} \sim T^{3/2}$ compared to the conductive heat flux $Q_{\mathrm{cond}} \sim T^{7/2}$ as the divertor temperature drops.

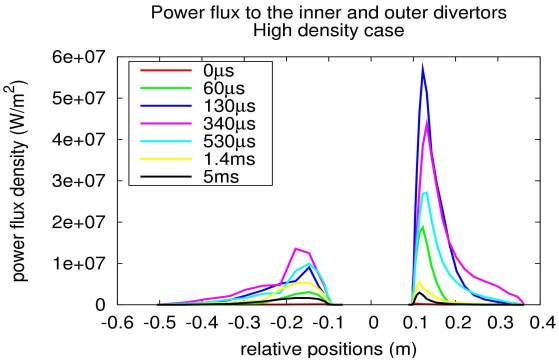

Figure 3: power deposition profiles on divertors for puffing rate $\dot{n}_{\mathrm{puff}} = 1.2 \cdot 10^{20}\,\mathrm{m}^{-2}\mathrm{s}^{-1}$

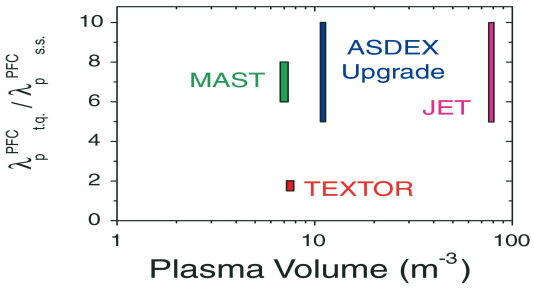

Figure 4: $\lambda_{\mathrm{t.q.}}/\lambda_{\mathrm{s.s.}}$ [1]

Fig. 3 shows the power deposition profiles along the inboard and outboard divertors for a case with high puffing rate, i.e. low divertor temperatures. It not only shows that the bulk of the heat pulse goes to the outboard divertor but also that it arrives there first (after $130\,\mu$s compared to $340\,\mu$s for the inner divertor). This time delay indicates that the better part of the heat pulse crosses the separatrix at the outboard side where connection lengths to the outboard divertor are short. The asymmetry then results from a non-linear feedback of the temperature to the transport coefficients (Eq. 1).

The figure also allows us to define the width λ of the power deposition profile to be the poloidal half width of the profile at the maximum power load. The power deposition width can be defined for the thermal quench ($\lambda_{\mathrm{t.q.}}$) as well as for the steady-state phase ($\lambda_{\mathrm{s.s.}}$). Generally, plasma disruptions exhibit a significant broadening of the power deposition profiles, i.e. $\lambda_{\mathrm{t.q.}}/\lambda_{\mathrm{s.s.}} > 1$ (Fig. 4). The same ratio of power deposition widths can be calculated for the simulated cases where we have to distinguish, however, between inboard and outboard divertors. The result is shown in Fig. 5. For low puffing rates, i.e. fully attached divertors, a significant broadening of the power deposition profiles is found, comparable to the experimentally observed broadening. The broadening here is strongest for the outboard divertor. With increasing puffing rate, however, both broadening factors drop until they reach a level where no significant broadening is seen. The drop in the broadening factors here is partly due to the increased steady-state profile width but mainly to the reduced width during the thermal quench. This reduction coincides with the regime of asymmetric power fluxes such that the power load onto the outboard divertor is increased both through the asymmetry in the power fluxes as well as through the suppression of the profile broadening. It remains to be checked how this relates to experimental findings

that generally show a clear profile broadening. A suppression of the profile broadening however could possibly raise power fluxes to the divertors during thermal quenches beyond acceptable levels and thereby pose a threat to the divertor structures. Further more elaborate numerical models as well as better experimental diagnostics and analysis is needed to clarify this point.

Discussion

We have studied the characteristics of the redistribution phase of thermal quenches by performing time dependent disruption simulations using the B2 SOLPS multifluid code. Based on an ASDEX Upgrade H-mode shot, a suite of steady-state equilibria have been calculated which differ by the physical conditions in the divertor regions, i.e. divertor temperatures and densities. Starting from these equilibria, thermal quenches have been simulated by switching on a strongly enhanced cross-field transport in heat and particle channels for ions and electrons following the model by Rechester and Rosenbluth [4]. The results have been compared to experimental findings.

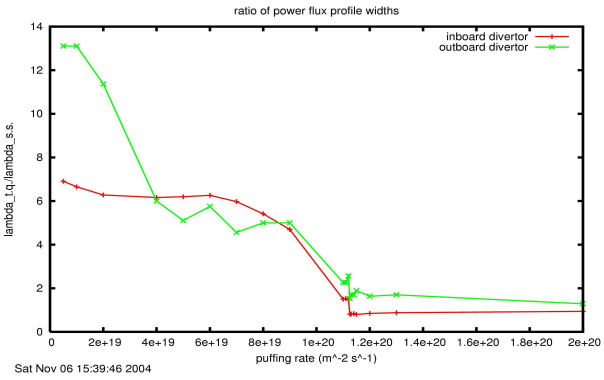

Figure 5: ratio of deposition widths $\lambda_{\mathrm{t.q.}}/\lambda_{\mathrm{s.s.}}$ vs. puffing rate $\dot{n}_{\mathrm{puff}}$

Our simulations show a clear dependence of the thermal quench characteristics on the pre-disruptive divertor conditions. Power flux timescales and widths are comparable to experimentally measured values for cases with low puffing rates, i.e. mostly attached divertors. For higher puffing rates, i.e. colder divertors, the simulations show a strong asymmetry in the power fluxes coupled with a suppression of the profile broadening which is not seen in experiments. An enhanced transport model may be needed, together with more precise experimental diagnostics, to resolve this discrepancy.

References

[1] Loarte, A. et al., ITER IAEA Fusion Energy Conference 2004, IAEA-CN-116 IT/P3-34 (2004)

[2] Braams, B.J., Contr. Plasma Phys. **36**, 276 (1996)

[3] Pereverzev, G.V. and Yushmanov, P.N., IPP-Report, IPP 5/98 (2002)

[4] Rechester, A.B. and Rosenbluth, M.N., Phys. Rev. Lett. **40**, 38 (1978)

[5] Pautasso, G. et al., EPS Conference on Plasma Phys., ECA **28G**, P-4.132 (2004)